Spectroscopic evidence for anisotropic *s*-wave pairing symmetry in MgB_2

P. Seneor,[1] C.-T. Chen,[1] N.-C. Yeh,[1] R. P. Vasquez,[2] L. D. Bell,[2] C. U. Jung,[3] Min-Seok Park,[3] Heon-Jung Kim,[3] W. N. Kang,[3] and Sung-Ik Lee[3]

[1]*Department of Physics, California Institute of Technology, Pasadena, California 91125*

[2]*Center for Space Microelectronics Technology, Jet Propulsion Laboratory, California Institute of Technology, Pasadena, Calfornia 91109*

[3]*National Creative Research Initiative Center for Superconductivity and Department of Physics, Pohang University of Science and Technology, Pohang 790-784, Republic of Korea*

(Received 10 September 2001; published 29 November 2001)

Scanning tunneling spectroscopy of superconducting MgB_2 ($T_c = 39$ K) were studied on high-density pellets and *c*-axis oriented films. The sample surfaces were chemically etched to remove surface carbonates and hydroxides, and the data were compared with calculated spectra for all symmetry-allowed pairing channels. The pairing potential (Δ_k) is best described by an anisotropic *s*-wave pairing model, with $\Delta_k = \Delta_{xy}\sin^2\theta_k + \Delta_z\cos^2\theta_k$, where θ_k is the angle relative to the crystalline *c*-axis, $\Delta_z \sim 8.0$ meV, and $\Delta_{xy} \sim 5.0$ meV.

DOI: 10.1103/PhysRevB.65.012505 PACS number(s): 74.50.+r, 74.20.Rp, 74.76.Db, 74.80.Bj

Since the discovery of superconductivity in MgB_2 at a superconducting transition temperature $T_c \sim 39$ K,[1] a number of papers[1–7] have suggested that this hole-doped layered superconductor[8–10] may be consistent with conventional BCS *s*-wave pairing. On the other hand, muon spin rotation (μSR) studies of MgB_2 have found that the temperature dependence of the magnetic penetration depth is suggestive of unconventional pairing symmetry with nodes in the superconducting order parameter.[11] To address the issue of the pairing symmetry in this new superconductor, possible complications by disorder or surface impurities must be considered. Indeed, recent x-ray photoemission spectroscopy (XPS) studies have revealed that $MgCO_3$ and $Mg(OH)_2$ exist on the surface of as-grown MgB_2.[12] It is, therefore, important to understand how these surface impurity phases may contribute to surface-sensitive experiments such as the scanning tunneling spectroscopy[4–6] (STS) and point-contact measurements[7] of the quasiparticle spectra. In particular, existing STS data on as-grown polycrystalline MgB_2 (Ref. 5) exhibited ''V-shape'' differential conductance (dI_{NS}/dV) vs voltage (V) plots near zero bias (i.e., the Fermi level E_F), with rounded ''humps'' rather than sharp peaks at the gap values ($V = \pm\Delta/e$) and large residual density of states (DOS) at E_F. Those spectra were fitted with an *s*-wave pairing potential Δ broadened by disorder parameterized as Γ, and a large ratio of $(\Gamma/\Delta) \sim 60\%$ was suggested.[5] For comparison, in cuprate superconductors the V-shape conductance spectra near E_F for quasiparticle tunneling along the *c* axis are known to be the signature of the $d_{x^2-y^2}$ pairing symmetry,[13–17] and strong directionality in the quasiparticle spectra has been observed.[13–15] In particular, a zero-bias conductance peak[18,19] (ZBCP) can occur if quasiparticles are incident close to the {110} nodal direction of the $d_{x^2-y^2}$-wave order parameter. Thus, should the pairing symmetry be unconventional, the observation of V-shape tunneling spectra in polycrystalline MgB_2 samples associated with certain grain orientations would be accompanied by frequent occurrence of ZBCP for other grain orientations. To date, no ZBCP has been found from vacuum tunneling studies of as-grown MgB_2.[4–6] However, a major concern presented by existing quasiparticle spectra is that the measured gap values vary widely, and that most values are smaller than that the BCS prediction.[4–7]

Our starting point for investigating the pairing symmetry of MgB_2 is to consider all the possible pairing channels based on group theory. The global symmetry group $\mathcal{G}$ of MgB_2 in its normal state can be expressed by $\mathcal{G} = \mathrm{U}(1) \times \mathcal{T} \times \mathrm{SU}(2) \times \mathcal{G}_{space}$, where U(1) is the electromagnetic gauge broken below T_c, $\mathcal{T}$ and SU(2) denote the time-reversal and spin-rotational symmetries that are generally preserved below T_c for spin-singlet Cooper pairs, and $\mathcal{G}_{space}$ is the space group D_{6h} for MgB_2. Given that the Cooper pairs in MgB_2 are spin-singlets[2] and that no other obvious symmetry-breaking fields exist below T_c except U(1), the possible pairing channels can be derived from the even-parity irreducible representations of D_{6h}. For a single-component superconductor, the relevant pairing channels can be further reduced to four one-dimensional (1D) even-parity irreducible representations in D_{6h}: A_{1g}, A_{2g}, B_{1g}, and B_{2g}. The pairing potentials Δ_k for these representations can be expressed as a function of the momentum $\vec{k}$ to the lowest order:

$$
\begin{aligned}
A_{1g}&: \Delta_k = \Delta_0, \quad (\text{isotropic } s)\\
&: \Delta_k = \Delta_0[1 + \epsilon\cos(6\phi_k)], \quad (\text{anisotropic } s)\\
&: \Delta_k = \Delta_{xy}\sin^2\theta_k + \Delta_z\cos^2\theta_k, \quad (\text{anisotropic } s)\\
A_{2g}&: \Delta_k = \Delta_0\sin^6\theta_k\sin(6\phi_k), \qquad (1)\\
B_{1g}&: \Delta_k = \Delta_0\cos\theta_k\sin^3\theta_k\sin(3\phi_k),\\
B_{2g}&: \Delta_k = \Delta_0\cos\theta_k\sin^3\theta_k\cos(3\phi_k).
\end{aligned}
$$

Here θ_k is the angle measured relative to $\hat{k}_z$, with $\hat{k}_z$ parallel to the crystalline c axis, and ϕ_k is measured relative to $\hat{k}_x$. In addition, $0 < \epsilon < 1$ and $\Delta_{xy} \neq \Delta_z$ for the anisotropic *s*-wave pairing potentials. The graphical representations of these different pairing potentials are illustrated in Figs. 1(a)–1(d).

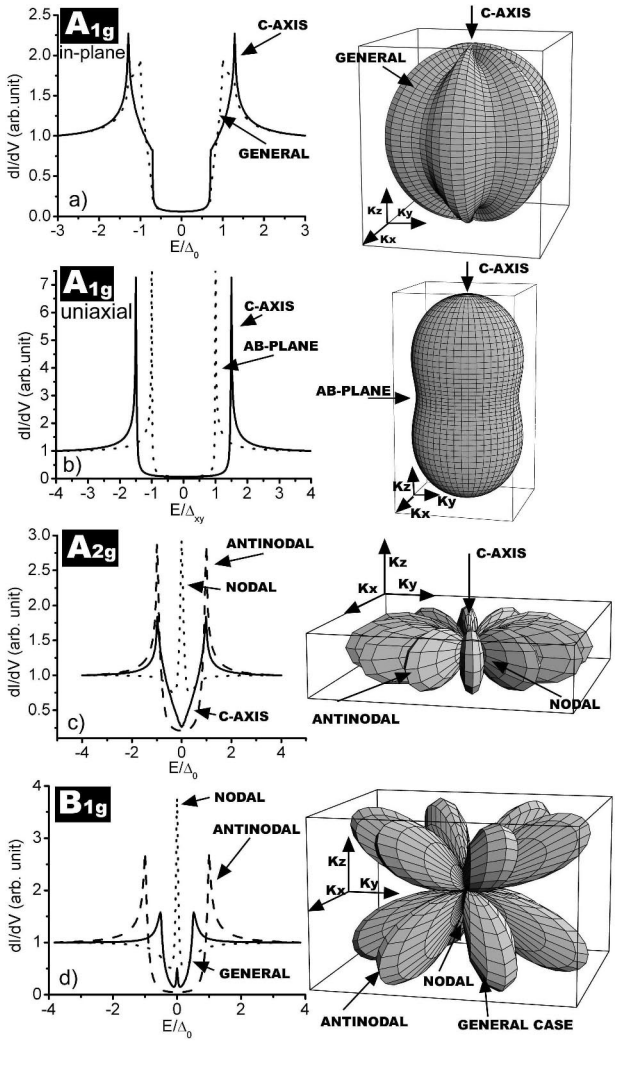

FIG. 1. Right panels: Graphical representations for possible order parameters permitted by the D_{6h} group symmetry and spin-singlet pairing. Left panels: Simulated differential conductance ($G_{NN}dI_{NS}/dV$) vs voltage (V) quasiparticle tunneling spectra at 4.2 K, assuming $\Delta_0=6.5$ meV, for the following 1D even-parity representations. (a) A_{1g}, anisotropic s wave with in-plane anisotropy; (b) A_{1g}, anisotropic s wave with uniaxial symmetry; (c) A_{2g}; (d) B_{1g}, or B_{2g} by rotating B_{1g} order parameter through an angle ($\pi/6$) relative to k_z.

Among different A_{1g} representations, the lowest-order possibilities include the isotropic s-wave order parameter, anisotropic s wave with six fold in-plane modulations, or anisotropic s wave with uniaxial symmetry, with the latter two illustrated in Figs. 1(a) and 1(b). The lowest-order A_{2g} representation consists of twelve ''lobes'' of alternating phases, and the phases are even under k_z inversion. For either B_{1g} or B_{2g} representation, the order parameter consists of twelve lobes with alternating phases, and the phases are odd under k_z inversion.

To obtain the quasiparticle spectra for all possible pairing channels with different Δ_k, we consider a crystalline plane with a normal vector $\hat{n}_k$ characterized by the parameters (θ_k,ϕ_k). Defining the direction of an incident quasiparticle relative to $\hat{n}_k$ by the parameters $\hat{l}(\theta_{in},\phi_{in})\equiv\hat{l}_{in}$, which explicitly considers the transverse momentum for the incident quasiparticles (i.e., a finite ''tunneling cone'') relative to $\hat{n}_k$, such that θ_{in} is primarily confined between $-\beta$ and β, and $0\leqslant\phi_{in}\leqslant 2\pi$, we can generalize the theory of Blonder-Tinkham-Klapwijk[18–20] (BTK) to three dimensions (3D), and compute the tunneling current I_{NS} as a function of the bias voltage V, temperature T, tunneling barrier strength Z, tunneling direction $\hat{n}_k$, and tunneling cone β:

$$I_{NS}=G_{NN}\int_0^{2\pi}d\phi_{in}\int_0^{\pi/2}d\theta_{in}\cos\theta_{in}e^{-(\theta_{in}^2/\beta^2)}\int dE_k \times[1+A-B]\times[f(E_k-eV)-f(E_k)]. \quad (2)$$

In Eq. (2), G_{NN} denotes the normal-state conductance, E_k is the quasiparticle energy, A and B represent the kernals for Andreev and normal reflection, respectively, and $f(E_k)$ is the Fermi function.[18,19] Thus, the differential conductance spectra dI_{NS}/dV vs V can be obtained for given $\hat{n}_k$ and Δ_k using Eqs. (1) and (2). The representative spectra for high-impedance tunneling barrier $Z=5$ are shown in the left panels of Figs. 1(a)–1(d).

Except for the A_{1g} representation, the spectral characteristics for all other representations exhibit strong directionality (i.e., dependence on the crystalline normal $\hat{n}_k$ relative to the average quasiparticle momentum), as manifested by calculated spectra in the right panels of Figs. 1(a)–1(d). It is clear that the ZBCP would have been a common occurrence in the tunneling spectra of MgB_2 pellets had the order parameter been one of the unconventional pairing channels (A_{2g},B_{1g},B_{2g}).

To compare the calculated results with experiments, we performed scanning tunneling spectroscopy on high-density pellets[21–23] and c-axis textured films of MgB_2 (Ref. 24) at 4.2 K. Both the pellets and c-axis films were fully characterized,[12,21–24] showing single-phased material with superconducting transition at $T_c=39.0$ K, sharp magnetization transition widths ($\Delta T_c<1$ K for the pellets and $\Delta T_c\sim 0.7$ K for the films), and nearly 100% bulk superconducting volume.[21–24] According to XPS studies on these samples,[12] the surface $MgCO_3$ and $Mg(OH)_2$ impurities on the as-grown MgB_2 could be mostly removed by chemical etching, with no discernible etch residues for the tunneling experiments.[12] Tunneling studies were conducted on the as-grown and etched MgB_2 pellets and films at 4.2 K, using a low-temperature scanning tunneling microscope. Spatially resolved tunneling spectra were taken on over 100 randomly oriented grains of each sample. On each grain, the spectra were taken under the vacuum tunneling condition and on an area approximately (200 nm$\times$200 nm) in size with nanoscale surface flatness. A large number of grains were studied on each sample to ensure sufficient statistical sampling of different $\hat{n}_k$ in pellets.

Representative tunneling spectra for a MgB_2 pellet after etching are shown in the main panel of Fig. 2(a), and those for the same sample before etching are given in the lower right inset. We note significantly improved spectra after etch-

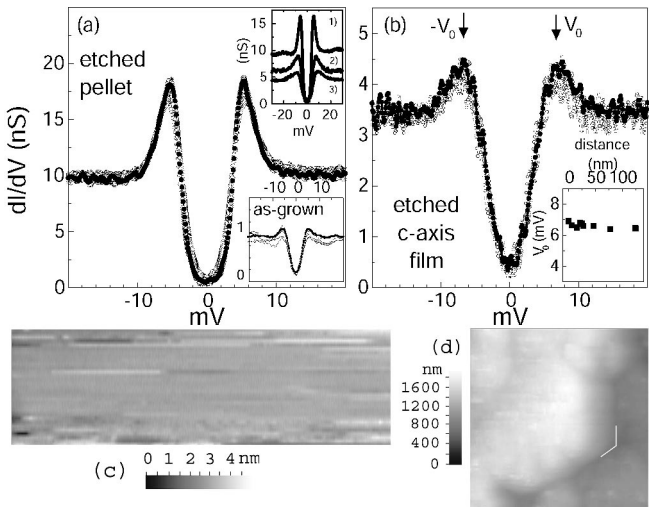

FIG. 2. (a) Spatially resolved tunneling spectra of a high-density MgB_2 pellet. The main panel and the lower right inset illustrate data taken at locations 10~15 nm apart within one grain after and before chemical etching, respectively. The upper right inset shows representative spectra on the etched pellet with different junction resistance at 20 mV: 1) 108 MΩ, 2) 179 MΩ, 3) 253 MΩ. The work function for these spectra is typically 0.1~1 eV. (b) A series of tunneling spectra on an etched c-axis film (main panel), showing long-range spatial homogeneity in the spectral peak-to-peak energies and a large junction resistance ~330 MΩ (inset). (c) An image of the surface topography of the etched sample over an area (196 nm×60 nm). The full scale for the height is 4.7 nm. (d) An atomic-force-microscope (AFM) image over an area (620 nm ×620 nm). The white lines indicate two grain boundaries forming an angle at ~120°.

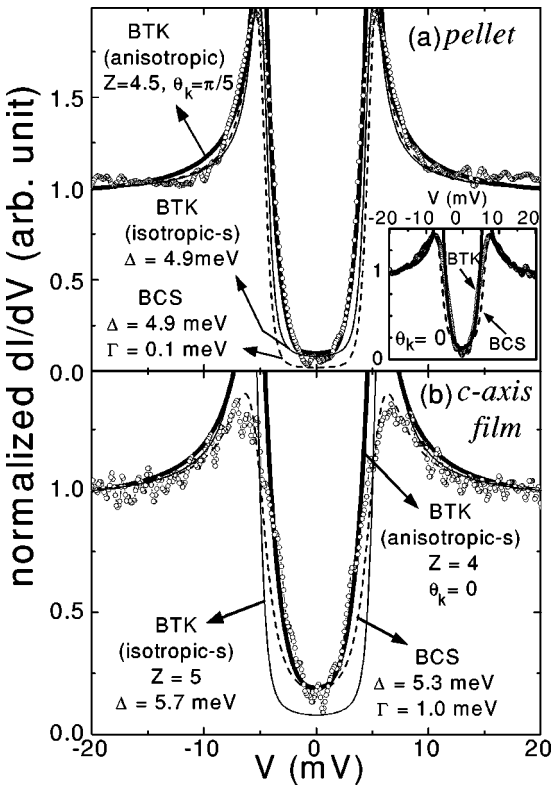

FIG. 3. BTK anisotropic and isotropic *s*-wave fitting, together with the isotropic BCS fitting to representative spectra of (a) an etched MgB_2 pellet, and (b) an etched c-axis film. Given empirical values of Δ_{xy} and Δ_z, the anisotropic s-wave fitting is only sensitive to the variation in θ_k and is insensitive to a wide range of β values that we have tested, from $(\pi/18)$ to $(\pi/2)$. The fitting curves shown have assumed the most general case with $\beta=\pi/2$.

ing, with long-range spatial homogeneity (>400 nm) within each grain, which correlated well with the long-range atomic flatness of the topography as exemplified in Figs. 2(c) and 2(d), and was in contrast to the strong spatial variations in both the spectra and topography of MgB_2 powder.[25] Furthermore, DOS nearly vanished at E_F, with a normalized value $[(dI_{NS}/dV)_{V=0}/(dI_{NS}/dV)_{V=20\ \mathrm{meV}}]\sim 2\%$. While the tunneling spectra were homogeneous within each grain (with lateral dimension ~ a few micrometers[22]), the gap values varied from grain to grain in the pellets, ranging from ~5 to ~8 meV. On the other hand, tunneling spectra of etched *c*-axis oriented films were homogeneous everywhere. Overall, no ZBCP was observed among over five hundred spectra taken on all samples. We, therefore, conclude that the pairing symmetry must be of the A_{1g} representation.

To identify the correct pairing potential under the A_{1g} representation in Eq. (1), we performed the BTK analysis for both anisotropic and isotropic *s*-wave pairing, as well as the isotropic BCS fitting to all spectra. The latter involved a disorder parameter Γ for an isotropic gap Δ with the density of states $\mathcal{N}(E)$ given by Ref. 26,

$$\mathcal{N}(E)=\mathrm{Re}[(E-i\Gamma)/\sqrt{(E-i\Gamma)^2-\Delta^2}]\propto dI_{NS}/dV.$$

For both BTK and BCS isotropic *s*-wave fitting, we notice several difficulties. First, the inclusion of the disorder-induced pair-breaking strength Γ alone cannot fully account for the spectral characteristics, particularly the linewidth and lineshape of the peaks, as manifested in Figs. 3(a) and 3(b). Second, significant variations in the supposedly isotropic pairing potential must be invoked to account for all data taken on the pellets. The variation was unlikely the result of bulk stoichiometric inhomogeneity because of the sharp superconducting transition width (<1 K) revealed in the magnetization measurement of our MgB_2 pellet. In other words, had the gap variation been the result of the grain-to-grain stoichiometric variation, we would have observed a very broad T_c distribution in the magnetization measurements, from ~39 K to ~24 K for the 5~8 meV gap variation. Given the quality of the spectra and topography of our well characterized sample surfaces, we suggest that the variation observed in the gap values of MgB_2 pellets is the result of different grain orientations relative to the incident quasiparticles. The single gap value in the *c*-axis oriented films further corroborates the notion of *k*-dependent pairing potential. More importantly, had the pairing symmetry been isotropic *s* wave, the $(2\Delta/k_BT_c)$ ratios deduced from our tunneling spectra would not have varied from ~2.5 to ~4.5 from grain to grain for T_c variation smaller than 1.0 K. In addition, to date there is no known theory for isotropic *s*-wave superconductors that can justify a $(2\Delta/k_BT_c)$ ratio smaller than the BCS value.

On the other hand, the electronic and structural anisotropy in the MgB_2 system can lead to anisotropic *s*-wave pairing, and, therefore, a $\vec{k}$-dependent pairing potential and a range of gap values in the STS studies of polycrystalline samples. Comparing the two possibilities of anisotropic s-wave pairing potentials depicted in Figs. 1(a) and 1(b), we note that an in-plane sixfold anisotropy would have resulted in a *c*-axis spectrum with a sharp peak at $\Delta_0(1+\epsilon)$ and complicated spectral curvatures in $\mathcal{N}(E)$ for $\Delta_0(1-\epsilon)<E<\Delta_0(1+\epsilon)$, as shown in Fig. 1(a). Such behavior was never seen in our data. In contrast, spectra derived from the order parameter in Fig. 1(b) appeared to be most consistent with our finding of smooth spectra on all samples, and with one maximum gap value at $\Delta_z \sim 8$ meV for the c-axis films.

Using the anisotropic *s*-wave pairing potential $\Delta_k = \Delta_{xy}\sin^2\theta_k + \Delta_z \cos^2\theta_k$, with the minimum gap $\Delta_{xy} \approx 5$ meV and the maximum gap $\Delta_z \approx 8$ meV determined empirically, we can consistently account for all experimental data on both pellets and *c*-axis films by varying one parameter θ_k. As exemplified in the main panel and inset of Fig. 3(a), the former is consistent with $\theta_k = (\pi/5)$ and the latter with $\theta_k = 0$. Similarly, the same pairing potential can also be applied to the *c*-axis film data with $\theta_k = 0$, as shown in the main panel of Fig. 3(b). Our empirical finding of a smaller in-plane gap value ($\Delta_{xy} < \Delta_z$) is consistent with the stronger in-plane Coulomb repulsion in MgB_2.[27] A similar anisotropic *s*-wave pairing scenario has been proposed to account for the thermodynamic and optical properties of MgB_2 wires,[28] and recent Raman scattering measurements on MgB_2 single crystals have also confirmed an anisotropic *s*-wave scenario.[29] Furthermore, a number of experimental reports including the upper critical field (H_{c2}) measurements,[30] high-resolution photoemission spectroscopy,[31] and electron spin resonance,[32] are all supportive of significantly anisotropic properties in the superconducting state of MgB_2.

In summary, we have investigated the possible pairing channels in MgB_2 based on group theory consideration, and have calculated the quasiparticle spectra using a generalized BTK theory for quasiparticle tunneling in 3D. Comparing the calculated results with spectra taken on fully characterized MgB_2 pellets and c-axis oriented films, we conclude that the order parameter of MgB_2 belongs to the A_{1g} representation of D_{6h} group, and is best described by an anisotropic *s*-wave pairing potential with uniaxial symmetry.

The research at Caltech was supported by NSF Grant No. DMR-0103045 and the Caltech President's Fund. Part of the work described in this paper was performed by the Center for Space Microelectronics Technology, Jet Propulsion Laboratory, and was sponsored by NASA. The work at Pohang University was supported by the Ministry of Science and Technology of Korea through the Creative Research Initiative Program.

[1] J. Nagamatsu, N. Nakagawa, T. Muranaka, Y. Zenitani, and J. Akimitsu, Nature (London) **410**, 63 (2001).
[2] H. Kotegawa, K. Ishida, Y. Kitaoka, T. Muranaka, and J. Akimitsu, cond-mat/0102334 (unpublished).
[3] S.L. Bud'ko, G. Lapertot, C. Petrovic, C.E. Cunningham, N. Anderson, and P.C. Canfield, Phys. Rev. Lett. **86**, 1877 (2001).
[4] G. Rubio-Bollinger, H. Suderow, and S. Vieira, Phys. Rev. Lett. **86**, 5582 (2001).
[5] G. Karapetrov, M. Iavarone, W.K. Kwok, G.W. Crabtree, and D.G. Hinks, Phys. Rev. Lett. **86**, 4374 (2001).
[6] A. Sharoni, I. Felner, and O. Millo, Phys. Rev. B **63**, 220508 (2001).
[7] H. Schmidt, J.F. Zasadzinski, K.E. Gray, and D.G. Hinks, Phys. Rev. B **63**, 220504 (2001).
[8] J. Kortus, I.I. Mazin, K.D. Belashchenko, V.P. Antropov, and L.L. Boyer, Phys. Rev. Lett. **86**, 4656 (2001).
[9] J.M. An and W.E. Pickett, Phys. Rev. Lett. **86**, 4366 (2001).
[10] W.N. Kang, C.U. Jung, K.H.P. Kim, M.-S. Park, S.Y. Lee, H.-J. Kim, E.-M. Choi, K.H. Kim, M.-S. Kim, and S.-I. Lee, Appl. Phys. Lett. **79**, 982 (2001).
[11] C. Panagopoulos, B.D. Rainford, T. Xiang, C.A. Scott, M. Kambara, and I.H. Inoue, cond-mat/0103060 (unpublished).
[12] R.P. Vasquez, C.U. Jung, M.-S. Park, H.-J. Kim, J.Y. Kim, and S.-I. Lee, Phys. Rev. B **64**, 052510 (2001).
[13] N.-C. Yeh, J.Y.T. Wei, C.-T. Chen, W.D. Si, and X.X. Xi, Phys. Rev. Lett. **87**, 087003 (2001).
[14] N.-C. Yeh, C.-T. Chen, G. Hammerl, J. Mannhart, S. Tajima, K. Yoshida, A. Schmehl, C.W. Schneider, and R.R. Schulz, cond-mat/0103205, Physica C **364-365**, 450 (2001).
[15] J.Y.T. Wei, N.-C. Yeh, D.F. Garrigus,and M. Strasik, Phys. Rev. Lett. **81**, 2542 (1998).
[16] C.C. Tsuei and J.R. Kirtley, Rev. Mod. Phys. **72**, 969 (2000), and references therein.
[17] D.L. VanHarlingen, Rev. Mod. Phys. **67**, 515 (1995), and references therein.
[18] C.R. Hu, Phys. Rev. Lett. **72**, 1526 (1994).
[19] Y. Tanaka and S. Kashiwaya, Phys. Rev. Lett. **74**, 3451 (1995).
[20] G.E. Blonder, M. Tinkham, and T.M. Klapwijk, Phys. Rev. B **25**, 4515 (1982).
[21] G.Y. Sung, *et al.*, cond-mat/0102498 (unpublished).
[22] C.U. Jung, M.-S. Park, W.N. Kang, M.-S. Kim, K.H.P. Kim, S.Y. Lee, and S.-I. Lee, Appl. Phys. Lett. **78**, 4157 (2001).
[23] C.U. Jung, M.-S. Park, W.N. Kang, M.-S. Kim, S.Y. Lee, and S.-I. Lee, Physica C **353**, 162 (2001).
[24] W.N. Kang, H.-J. Kim, E.-M. Choi, C.U. Jung, and S.-I. Lee, Science **292**, 1521 (2001).
[25] F. Giubileo, D. Roditchev, W. Sacks, R. Lamy, and J. Klein, cond-mat/0105146 (unpublished).
[26] R.C. Dynes, V. Narayanamurti, and J.P. Garno, Phys. Rev. Lett. **41**, 1509 (1978).
[27] K. Voelker, V.I. Anisimov, and T.M. Rice, cond-mat/0103082 (unpublished).
[28] S. Haas and K. Maki, cond-mat/0104207 (unpublished).
[29] J.W. Quilty, S. Lee, A. Yamamoto, and S. Tajima, cond-mat/0107216 (unpublished).
[30] S.L. Bud'ko, V.G. Kogan, and P.C. Canfield, cond-mat/0106577 (unpublished).
[31] S Tsuda, T. Yokoya, T. Kiss, Y. Takano, K. Togano, H. Kitou, H. Ihara, and S. Shin, cond-mat/0104489 (unpublished).
[32] F. Simon *et al.*, Phys. Rev. Lett. **87**, 047002 (2001).